Published by :
http://www.ijert.org

International Journal of Engineering Research & Technology (IJERT)
ISSN: 2278-0181
Vol. 12 Issue 07, July-2023

MHD Boundary Layer Flow and Heat Transfer to Sisko Nanofluid Over a Nonlinear Stretching Sheet

Ch. Vittal [*1], Vijayalaxmi Tankasala[2], P. Ashok[3], S. Renuka[4], M. Chenna Krishna Reddy[3]
1*.Department of Mathematics, University College of Science, Saifabad, Osmania University, Hyderabad-500007, Telangana, India.
2. Department of Mathematics, NTR Govt Degree College, Mahabubnagar-509001, Telangana, India.
3. Department of Mathematics, Osmania University, Hyderabad-500007, Telangana, India.
4. Department of Mathematics, Nizam College, Osmania University, Hyderabad-500007, Telangana, India.

Abstract - The steady two-dimensional magneto hydrodynamic boundary layer flow and heat transfer to a Sisko nanofluid over a non-linear stretching surface has been investigated in the concerned study. The governing partial differential equations are reduced to a system of nonlinear ordinary differential equations using with appropriate similarity variables and solved numerically by using Runge-Kutta fourth order method along with shooting technique. The physical significance of the flow features, heat and mass transfer characteristics for different values of the parameters on the velocity, temperature and nanoparticle volume fraction profiles are discussed through graphical interpretations. The impingement of physical parameters on local skin friction coefficient, and rate of heat transfer are shown in tabulated form.

Keywords: Sisko fluid, heat transfer, MHD, nanofluid, nonlinear stretching sheet, Brownian motion, thermophoresis.

1. INTRODUCTION:

The boundary layer flow over a stretching surface is often encountered in some engineering disciplines. In particular, the flow induced by a stretching boundary is important in the extrusion processes in plastic and metal industries. Magyari and Keller[1] was first investigated the stretching problem of an incompressible fluid over a permeable wall. On the other hand, Gupta and Gupta[2]have mentioned that the stretching of the sheet may not necessarily be linear. In view of this Vajravelu[3] studied the flow and heat transfer in a viscous fluid over a nonlinear stretching sheet. Bhargava et al[4] examined the flow of a micro polar fluid over a nonlinear stretching sheet. Recently, Prasad et al[5] studied the heat transfer analysis with the effect of mixed convection over a nonlinear stretching surface with variable fluid properties. Keeping this in view, the effects of various parameters on the two dimensional flow towards a nonlinearly stretching sheet have been studied by many authors[6-9].

The Sisko fluid model has much significance due to its adequate description of many non- Newtonian fluids over the most important range of shear rates. Three parametric Sisko model can be considered as a generalization of Newtonian and power-law fluids which predicts both dilatants and pseudo plastic nature of fluid. The Sisko fluid model was originally proposed for high shear rate measurements on lubricating greases[10]. The three constants in the model can be chosen with great ease for specific fluid and model is found to be good in predicting the shear thinning and shear thickening behaviours. For the reason of their brilliant combined wetting and diffusing nature, Sisko nanofluids are also essential for the production of nanostructured materials. Khan and Shahzad[11]developed the boundary layer equations for Sisko fluid over a flat stretching sheet and obtained the analytical solutions for only integral values of the power-law index. Malik et al[12] have studied the flow and heat transfer in Sisko fluid with convective boundary condition over a non-isothermal nonlinearly stretching sheet in the presence of a uniform transverse magnetic field. Nonlinear radiative stagnation-point flow and heat transfer to Sisko fluid past a stretching cylinder in the presence of convective boundary conditions has been

International Journal of Engineering Research & Technology (IJERT)
ISSN: 2278-0181
Vol. 12 Issue 07, July-2023

analyzed by Khan et al[13] Mallik et al[14] provided a numerical investigation on the partial slip effects on the flow and heat transfer of an incompressible Sisko fluid over a nonlinear stretching sheet and stretching cylinder with variable thermal conductivity.

A nanofluid is a fluid possessing nanometer sized particles (1-100 nm diameters), called nanoparticles. The concept of nanofluid, has been advanced by Choi[15]through an innovative technique that uses a mixture of solid nanoparticles (Au, Ag, Cu metals, CuO, TiO_2 and Al_2O_3) having higher thermal conductivity and the base fluids (conventional liquids like water, engine oil, toluene, ethylene glycol etc.) of lower thermal conductivity so as to develop advanced heat transfer fluids with substantial augmentation of thermal conductivities. In other words, highest feasible thermophysical properties at the smallest feasible concentrations can be accomplished by uniform dispersion and stable suspension of nanoparticles in base fluids. Xuan and Li[16]implemented pure copper particles in the study of convective heat transfer and flow features of nanofluids. They found in their study that the volume fraction, the particle dimensions and material properties play significant role to achieve a substantial augmentation of heat transfer and viscosity.

Experimental studies have confirmed that with 1-5% volume of solid metallic or metallic oxide particles, the effective thermal conductivity of the resulting mixture can be enhanced by 20% compared to that of the base fluid[17-19]. The boundary layer flow problems involving nanofluids have been studied by many researchers[20-22]in recent years.

The study of magneto-hydrodynamic (MHD) flow of an electrically conducting fluid is of considerable interest in modern metallurgical and metal-working processes. The process of fusing of metals in an electrical furnace by applying a magnetic field and the process of cooling of the wall inside a nuclear reactor containment vessel are good examples of such fields[23]. Some important applications of radiative heat transfer include MHD accelerators, high temperature plasmas, power generation systems and cooling of nuclear reactors. Many processes in engineering areas occur at high temperatures and knowledge of radiation heat transfer becomes very important for the design of pertinent equipment[24]. In controlling momentum and heat transfers in the boundary layer flow of different fluids over a stretching sheet, applied magnetic field may play an important role[25]. Kumaran et al[26]investigated that magnetic field makes the streamlines steeper which results in the velocity boundary layer being thinner. The heat transfer analysis of boundary layer flow with radiation is also important in electrical power generation, astrophysical flows, solar power technology, space vehicle re-entry and other industrial areas. Raptis et al[27] reported the effect of thermal radiation on the MHD flow of a viscous fluid past a semi-infinite stationary plate.

Recently, Masood Khan, Rabia Malik et.al[28] investigated the steady heat and mass transfer mechanisms in a MHD Sisko nanofluid flow over a nonlinear stretching surface. The main emphasis of current paper deals with the two dimensional steady heat and mass transfer mechanisms in a MHD Sisko nanofluid flow over a nonlinear stretching surface in the presence of convective boundary condition. To achieve this study the suitable transformation is used to transform the partial differential equations to a system of ordinary differential equations together with boundary Conditions the resulting system of ordinary differential equations are solved using the well-known Runge-Kutta technique along with shooting method.

2. MATHEMATICAL FORMULATION:

Consider the laminar, two-dimensional, steady flow and heat transfer of the Sisko nanofluid in the region $y > 0$ driven by a sheet stretching with power-law velocity $U = cx^n$, where *c* represents a non-negative real number and $n > 0$ represents the stretching rate of the sheet. Thestretching sheet is assumed to be coinciding with the *x*- axis while the *y*-axis is perpendicular to the plane of the sheet. A hot fluid with temperature T_f is utilized to heat up or cool down the surface of the sheet (to be determined later) by convective heat transfer mode, which provides the heat transfer coefficienth_f. We assume the uniform nanoparticle volume fraction of the surface of the stretching sheet is C_w, whereas the ambient temperature and nanoparticle volume fraction are T_∞andC_∞ respectively. Under these assumptions along with boundary layer approximation the system of equations which governs the forced convective boundary layer flow is given by

$$\frac{\partial u}{\partial x} + \frac{\partial v}{\partial y} = 0 \ldots\ldots (1)$$

International Journal of Engineering Research & Technology (IJERT)
ISSN: 2278-0181
Vol. 12 Issue 07, July-2023

$$u\frac{\partial u}{\partial x}+v\frac{\partial u}{\partial x}=\frac{a}{\rho}\frac{\partial^2 u}{\partial y^2}-\frac{b}{\rho}\frac{\partial}{\partial y}\left(\frac{\partial u}{\partial y}\right)^n-\frac{\sigma}{\rho}B_0^2u\text{..... (2)}$$

$$u\frac{\partial T}{\partial x}+v\frac{\partial T}{\partial y}=\alpha\frac{\partial^2 T}{\partial y^2}+\tau\left[D_B\frac{\partial C}{\partial y}\frac{\partial T}{\partial y}+\frac{D_T}{T_\infty}\left(\frac{\partial T}{\partial y}\right)^2\right]\text{..... (3)}$$

$$u\frac{\partial C}{\partial x}+v\frac{\partial C}{\partial y}=D_B\frac{\partial^2 C}{\partial y^2}+\frac{D_T}{T_\infty}\frac{\partial^2 T}{\partial y^2}\text{ ..... (4)}$$

Here u and v denotes the components of velocity along the x and y directions, $B(x)=B_0x^{\frac{n-1}{2}}$represents the non-uniform magnetic field,$\nu\left(=\frac{\mu}{\rho_f}\right)$stands for kinematic viscosity, $\rho_f$for density of the base liquid, T for temperature, C for Nanoparticle volume fraction, $\tau\left(=\frac{(\rho c)_p}{(\rho c)_f}\right)$ is the ratio between the effective heat capacity of the nanoparticle material and heat capacity of the fluid, D_T for thermophoresis diffusion constant, $D_B$for Brownian diffusivity constant,T for temperature,C for Nanoparticle volume fraction, $\nu\left(=\frac{\mu}{\rho_f}\right)$stands for kinematic viscosity, $\alpha\left(=\frac{k}{\rho c_p}\right)$is the effective thermal diffusivity, k is the thermal conductivity of the fluid, ρ is the fluid density, c_p is the specific heat.

The associated boundary conditions are

$$\left.\begin{array}{c}u(x,y)=U_w(x),v(x,y)=0,-k\frac{\partial T(x,y)}{\partial y}=h_1\left(T_f-T(x,y)\right),D_B\frac{\partial C}{\partial y}+\frac{D_T}{T_\infty}\frac{\partial T}{\partial y}aty=0\\ u\to 0,T\to T_\infty,C\to C_\infty asy\to\infty\end{array}\right\}\quad(5)$$

And $U_w(x)=cx^n$ here c shows the rate of the stretching surface, T_f the temperature of the stretching surface, n the power-law index, T_∞ for ambient fluid temperature, C_∞ the ambient fluid concentration,

Introducing the following similarity transformations

$$\left.\begin{array}{c}u=Uf'(\eta),v=-URe_b^{\frac{1}{n+1}}\frac{1}{n+1}[\{s(2n-1)+1\}f(\eta)+\{s(2-n)-1\}\eta f'(\eta)],\\ \theta(\eta)=\frac{T-T_\infty}{T_f-T_\infty},\eta=\frac{y}{x}Re_b^{\frac{1}{n+1}},\phi(\eta)=\frac{C-C_\infty}{C_\infty}.\end{array}\right\}\text{....(6)}$$

By using above similarity transformations the equations (1), (2), (3) and (4) reduces to

$$Af'''+n(-f'')^{n-1}f'''+\left(\frac{s(2n-1)+1}{n+1}\right)ff''-s(f')^2-Mf'=0\text{..... (7)}$$

$$\theta''+Pr\left(\frac{s(2n-1)+1}{n+1}\right)f\theta'+Nb\theta'\phi'+Nt\theta'^2=0\text{..... (8)}$$

$$\phi''+LePr\left(\frac{s(2n-1)+1}{n+1}\right)f\phi'+\frac{Nt}{Nb}\theta''=0\text{ ..... (9)}$$

and the boundary conditions (5) are reduces to

$$\left.\begin{array}{c}f[0]=0,f'[0]=1,\ \theta'[0]=-\gamma\left[1-\theta[0]\right],Nb\phi'[0]+Nt\theta'[0]=0,\\ f'[\infty]\to 0,\ \theta[\infty]\to 0,\ \phi[\infty]\to 0.\end{array}\right\}\text{..... (10)}$$

Where prime denotes the differentiation with respect to η. $A\left(=\frac{Re_b^{\frac{1}{n+1}}}{Re_a}\right)$ is the material parameter of the Sisko nanofluid, $Pr\left(=\frac{xU}{\alpha}Re_b^{\frac{1}{n+1}}\right)$and $\gamma\left(=\frac{h_f}{k}xRe_b^{\frac{1}{n+1}}\right)$ are denotes the generalized Prandtl number and the generalized Biot number respectively, with $\gamma\to\infty$, the convective boundary condition reduces to the uniform surface temperature boundary condition, ,$Nt=$

International Journal of Engineering Research & Technology (IJERT)
ISSN: 2278-0181
Vol. 12 Issue 07, July-2023

$\frac{\tau D_T(T_f - T_\infty)}{T_\infty \alpha}, Nb = \frac{\tau D_B(C_w - C_\infty)}{\alpha}$ and $Le = \frac{\alpha}{D_B}$ represent the thermophoresis parameter, Brownian motion parameter and Lewis number, respectively.

Expressions for the local skin friction co-efficient C_{fx}, local Nusselt number Nu_x and local Sherwood number Sh_x are defined as,

$$C_{fx} = \frac{2\tau_w}{\rho U_m^2}, Nu_x = \frac{x q_w}{k_\infty (T_m - T_\infty)}, \; Sh_x = \frac{x q_m}{D_B (C_m - C_\infty)} \quad \text{..... (11)}$$

Where k_∞ is the thermal conductivity of the nanofluid, in which wall shear stress τ_w, q_w and q_m are the heat and mass flux, respectively given by

$$\left.\begin{aligned} \tau_w &= \eta_0 \left(\left(a + b \left| \frac{\partial u}{\partial y} \right|^{n-1} \right) \frac{\partial u}{\partial y} \right)_{y=0} \\ q_w &= -k_\infty \left(\frac{\partial T}{\partial y} \right)_{y=0} \\ q_m &= -D_B \left(\frac{\partial C}{\partial y} \right)_{y=0} \end{aligned} \right\} \text{..... (12)}$$

Using Eqs (6) and (7), the dimensionless parameters can be written in terms of the output of the local-similarity solutions as:

$$\left.\begin{aligned} Re_x^{\frac{1}{n+1}} C_{fx} &= A f''(0) - (-f''(0))^n, \\ Re_x^{-\frac{1}{n+1}} Nu_x &= -\theta'(0), Re_x^{-\frac{1}{n+1}} Sh_x = -\phi'(0). \end{aligned} \right\} \text{..... (13)}$$

Where $Re_x = \frac{U_m(x) x}{\nu}$ is local Reynolds number

3. NUMERICAL RESULTS AND DISCUSSION:

This section deals with the theoretical and graphical behaviour of different physical quantities which are involving in the present flow problem. The set of equations (10) - (12) are highly nonlinear and coupled hence it cannot be solved analytically. The numerical solutions of equations (10) - (12) subject to the boundary conditions (13) are obtained using an efficient numerical shooting technique with a fourth order Runge-Kutta scheme. For the purpose of discussing to provide physical insight into the present problem, comprehensive numerical computations are carrying out for various values of the flow parameters which describe the flow characteristics and the results are illustrated graphically. For computational purposes, the reason of integration η is consider as 0 to η_∞ is equivalent to (8), where η_∞ corresponds to $\eta \to \infty$ which lies very well outside the momentum and thermal boundary layer. The present results are compared with that of Masood Khan[28], Khan and Pop[29], Wang[30], Gorla[31]and found that were in good agreement between those and presented in table 1.A representative set of graphical results for the velocity, temperature and nanoparticle volume fraction as well as skin friction, local Nusselt number and local Sherwood number is present and discuss for different flow parameter values.

Table I. Comparison of the present results of local Nusselt number -θ'(0) for the case of Newtonian fluid for *Nt=Nb=R=γ=Le=M=0* with the results of, Masood Khan[28], Khan and Pop[29], Wang[30], Gorla[31].

International Journal of Engineering Research & Technology (IJERT)
ISSN: 2278-0181
Vol. 12 Issue 07, July-2023

Pr	Present study	Masood Khan [28]	Khan and Pop [29]	Wang [30]	Gorla [31]
0.7	0.453932	0.45392	0.4539	0.4539	0.5349
2.0	0.911358	0.91135	0.9113	0.9114	0.9114
7.0	1.895403	1.89543	1.8954	1.8954	1.8905
20.0	3.353904	3.35395	3.3539	3.3539	3.3539

Figures1(a)-1(b),2(a)-2(b) and 3(a)-3(b) shows the effect of the material parameter of the Sisko fluid (*A)*, on velocity, temperature and concentration profiles for the power-law index $n = 1$ and $n = 2$, respectively. It is observed that for increases in the value of material parameter (*A*), the dimensionless velocity and dimensionless concentration profiles increases for both cases. The temperature distribution is decreases with an increasing material parameter (*A*) for both cases.

Figures 4(a)-4(b), 5(a)-5(b), 6(a)-6(b) purports the velocity, temperature and concentration profiles for different values of magnetic parameter *M* in the cases of power-law index $n = 1$ and $n = 2$, respectively. It is inferred from this figures that increasing values of magnetic parameter *M* reduces the fluid velocity which causes the momentum boundary layer to shrink in both cases. It is acknowledging the fact that the transverse magnetic field in interaction with conducting nanofluid develops a retarding force called Lorentz force which decelerates the fluid motion. We would like to remark here that unless until the magnetic field were applied to the conducting fluid it would not have been opposed by Lorentz force so that the deceleration of fluid motion would not have been accomplished. However, the deceleration is well occasioned for higher strength of magnetic field. It implicates that increasing values of *M* enhances the fluid temperature leading to thicker thermal boundary layer in the flow domain in both cases.

The effects of the non-linear stretching parameter *s* on velocity, temperature and concentration profiles are shown in figures 7(a)-7(b), 8(a)-8(b), 9(a)-9(b) of power-law index $n=1$ and $n=2$ respectively. As increasing nonlinear stretching sheet parameter *s* decelerate the fluid velocity and temperature profile. It can be noticed that concentration profile increases as increasing in the non-linear stretching sheet parameter *s*. Furthermore, the temperature and concentration profiles are dependent on the non-linear stretching sheet parameter. The effect of power-law parameter *n* on velocity and temperature shows the decreasing nature where as it shows increasing nature in case of concentration profile when the value of *n* goes up. Fig. 10(a) and 10(b) represents the influence of power-law index 'n' on velocity profile $f'(\eta)$ for the case of shear thinning ($n < 1$) and shear thickening ($n > 1$) fluids. It is clearly observed that the velocity profile is diminishes with increase of power-law index '*n*' which results in reduction of boundary layer thickness for both the shear thinning and thickening fluids. In addition, the thickness of boundary layer is higher for shear thinning ($n < 1$) fluids than that of shear thickening ($n > 1$) fluids. The effect of the power-law index '*n*' on temperature profile $\theta(\eta)$ are depicted in Fig. 11(a) and 11(b) reveals the increment in power-law index causes the diminishes the temperature but the reverse trend is depicted in concentration profile which we can observe from the figures 12(a) and 12(b) for the both shear thinning ($n < 1$) and shear thickening ($n > 1$) fluids.

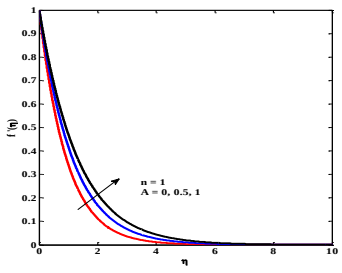

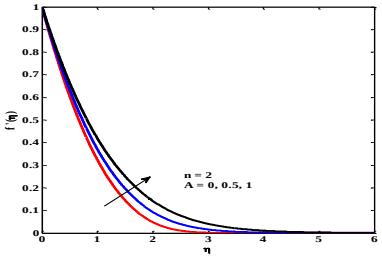

International Journal of Engineering Research & Technology (IJERT)
ISSN: 2278-0181
Vol. 12 Issue 07, July-2023

Fig. 1(a), 1(b).Velocity profile for *A*.

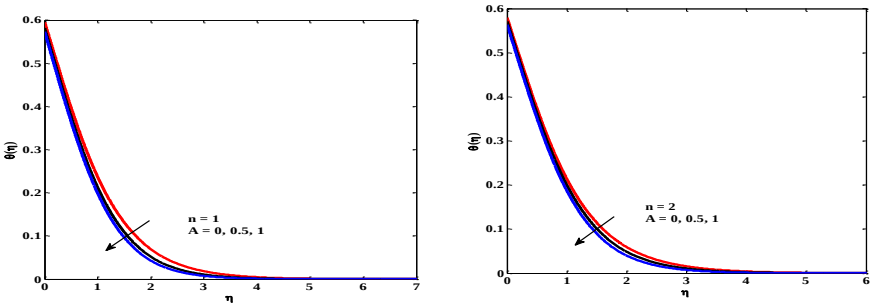

Fig. 2(a), 2(b).Temperature profile for *A*.

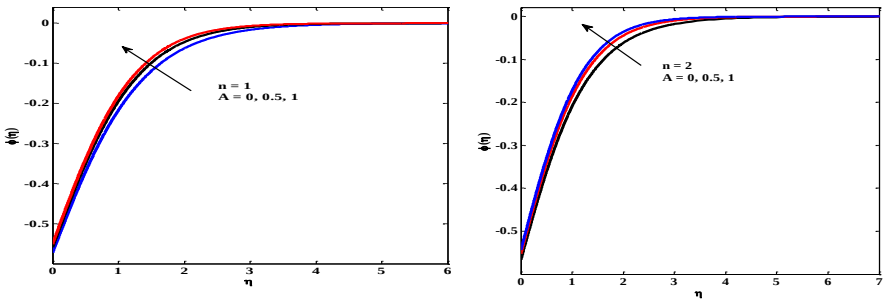

Fig. 3(a), 3(b).Concentration profile for *A*.

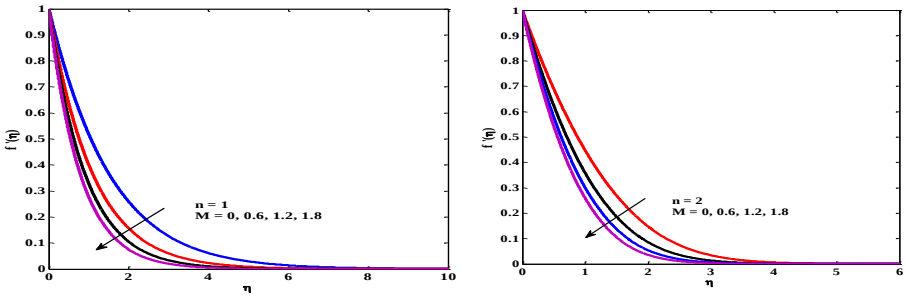

Fig. 4(a), 4(b).Velocity profile for *M*.

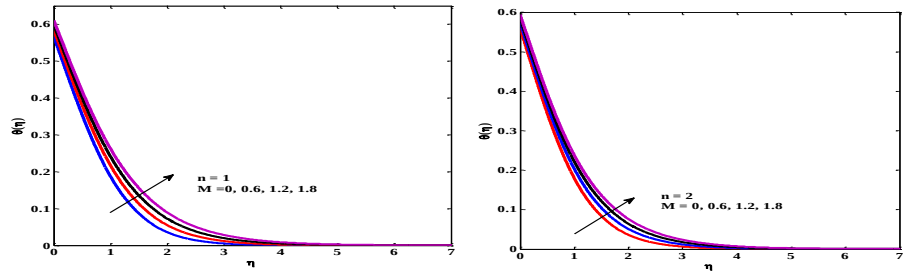

Fig. 5(a), 5(b).Temperature profile for *M*.

International Journal of Engineering Research & Technology (IJERT)
ISSN: 2278-0181
Vol. 12 Issue 07, July-2023

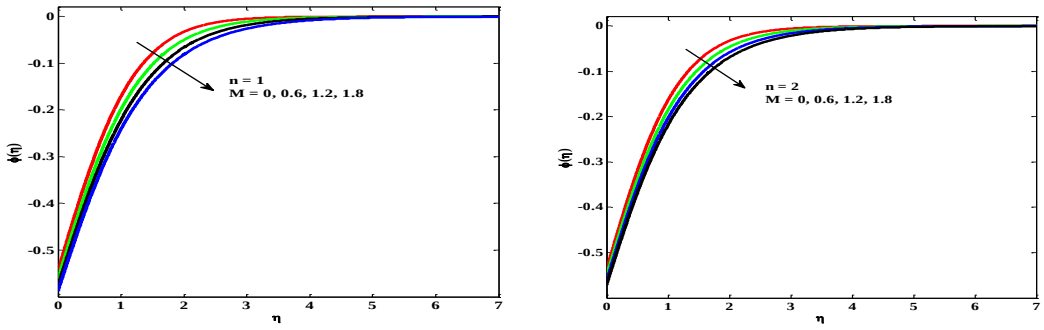

Fig. 6(a), 6(b).Concentration profile for *M*.

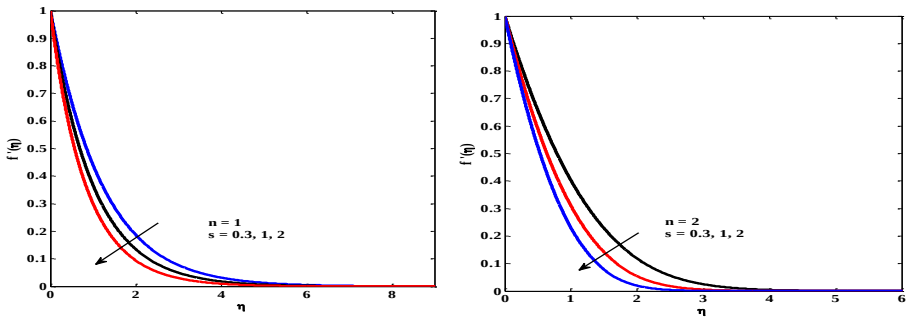

Fig. 7(a), 7(b).Velocity profile for *s*.

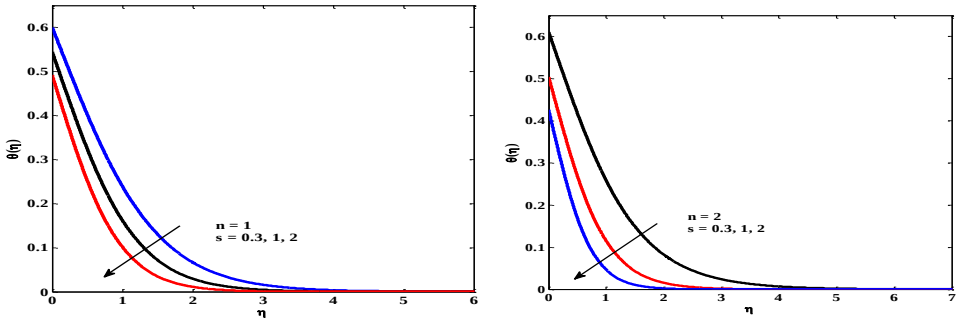

Fig. 8(a), 8(b).Temperature profile for *s*.

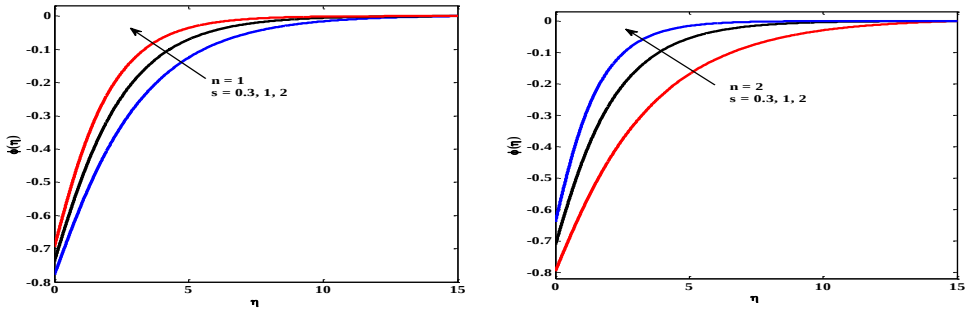

Fig. 9(a), 9(b).Concentration profile for *s*.

International Journal of Engineering Research & Technology (IJERT)
ISSN: 2278-0181
Vol. 12 Issue 07, July-2023

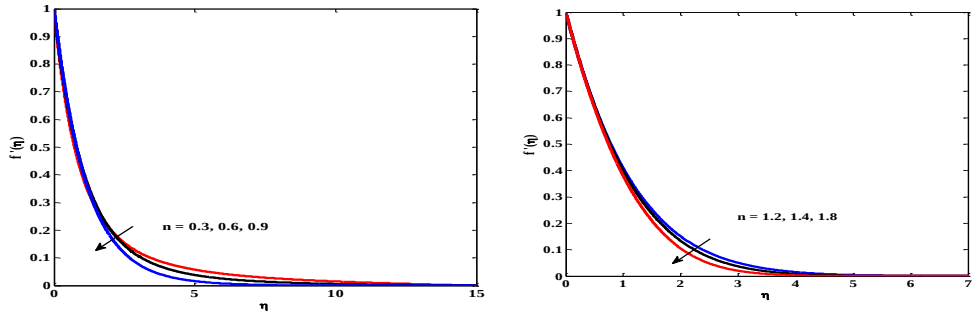

Fig. 10(a), 10(b).Velocity profile for *n*.

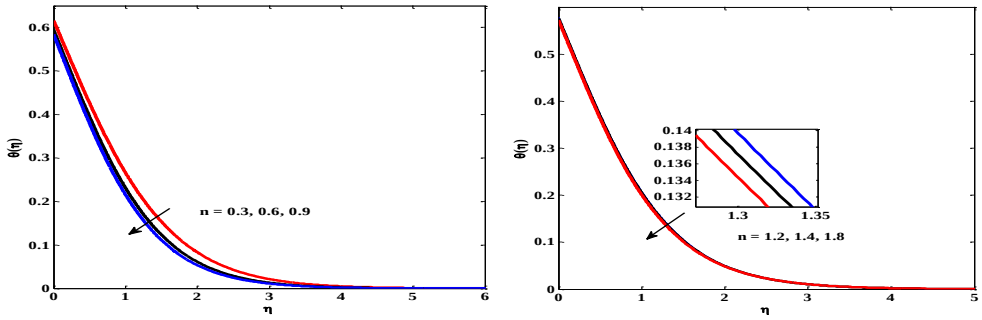

Fig. 11(a), 11(b).Temperature profile for *n*.

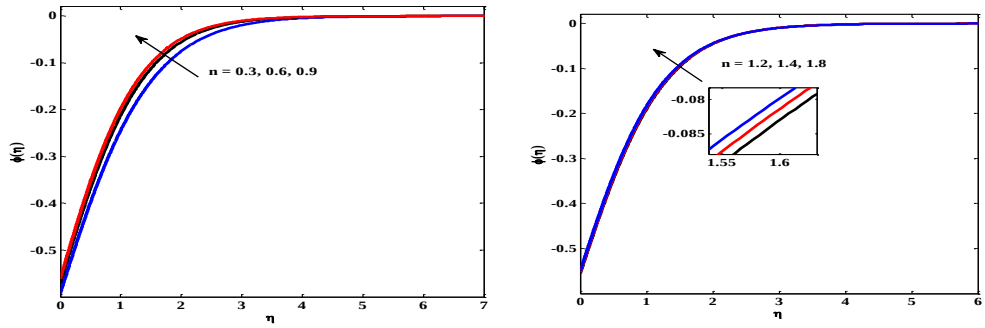

Fig. 12(a), 12(b).Concentration profile for *n*.

The influence of Biot number (γ) on temperature and concentration profiles are presented in figures 13(a)-13(b) and 14(a)-14(b) for the power-law index $n = 1$ and $n = 2$, respectively . We know that for high Biot number (γ) convective heating enhances and the isothermal surface $(i.e\theta(0) = 1)$ is reproduced as $\gamma \to \infty$. Indeed, higher generalized Biot number shows elevated internal thermal resistance of the surface than the boundary layer thermal resistance. It can be noticed that temperature and concentration profiles increases as increasing in the Biot number γ in both cases. The variation of the concentration profiles $\phi(\eta)$for different values of the Lewis number *Le* are shown in Figs. 15(a) and 15(b) for the power-law index $n = 1$ and $n = 2$, respectively. Generally Lewis number, is the ratio of thermal diffusivity to mass diffusivity, is used to characterize fluid flows where there is simultaneous heat and mass transfer by convection. It is noticed that the concentration profile enhances with an increase in *Le*.

Figures 16(a)-16(b), 17(a)-17(b) shows the effect of Brownian motion parameter *Nb* on temperature and concentration profiles for the power-law index $n = 1$ and $n = 2$ respectively. It is observed from figures that increasing values of Brownian motion parameter *Nb* enhances the temperature profile in both cases. It is also noticed that the concentration decreases by accelerating the

International Journal of Engineering Research & Technology (IJERT)
ISSN: 2278-0181
Vol. 12 Issue 07, July-2023

Brownian motion parameter *Nb* in both cases. This holds practically because with increase in *Nb* the random motion collusion of the macroscopic particles of the fluid increases.

Figures 18(a)-18(b), 19(a)-19(b) reflects the effect of Thermophoresis parameter *Nt* on temperature and concentration profiles for the power-law index $n = 1$ and $n = 2$ respectively. Thermophoresis mechanism in which small particles are pulled away from hot surface to cold surface due to this the transportation temperature of the fluid arises. Therefore the effect of Thermophoresis parameter *Nt* is to enhance the temperature profile in both cases. It can be observed that an enhancement in the Thermophoresis parameter *Nt* produces a force which leads to the moment of nano particles from a hot region to cold region and hence the concentration profile increases with an increasing in the values of Thermophoresis parameter *Nt* in both cases.

Figures 20(a)-20(b),21(a)-21(b) describes the behaviour of Prandtl number *Pr* on the temperature, concentration profiles for the power-law index $n = 1$ and $n = 2$ respectively. It is noticed that increasing values of *Pr* decrease the thermal diffusivity there by belittles the fluid temperature which in turn reduces thermal boundary layer thickness. It is also noticed that the concentration profile decreases by uplifting the Prandtl number *Pr* and hence decreases concentration boundary layer thickness.

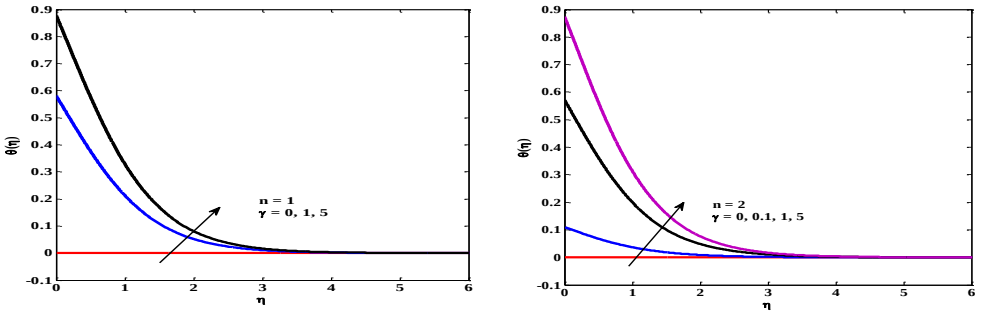

Fig. 13(a), 13(b). Temperature profile for γ.

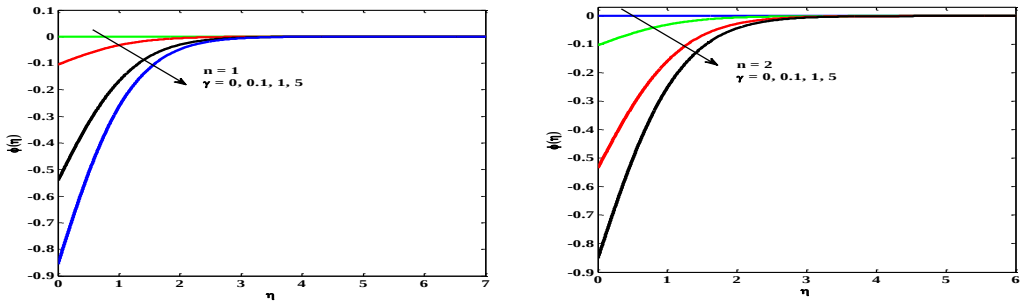

Fig. 14(a), 14(b). Concentration profile for γ.

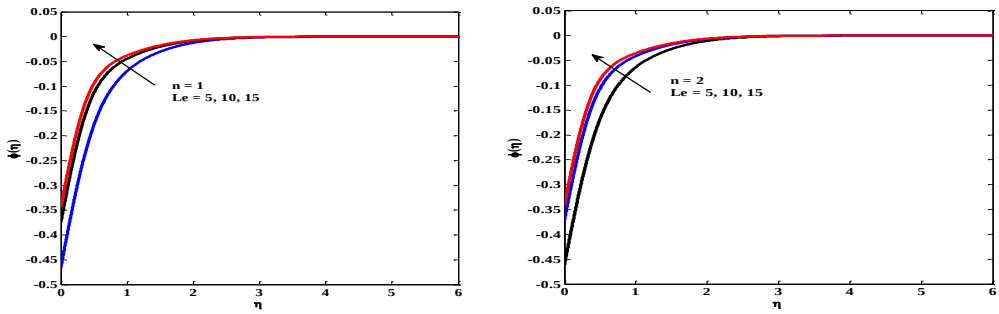

International Journal of Engineering Research & Technology (IJERT)
ISSN: 2278-0181
Vol. 12 Issue 07, July-2023

Fig. 15(a), 15(b).Concentration profile for *Le*.

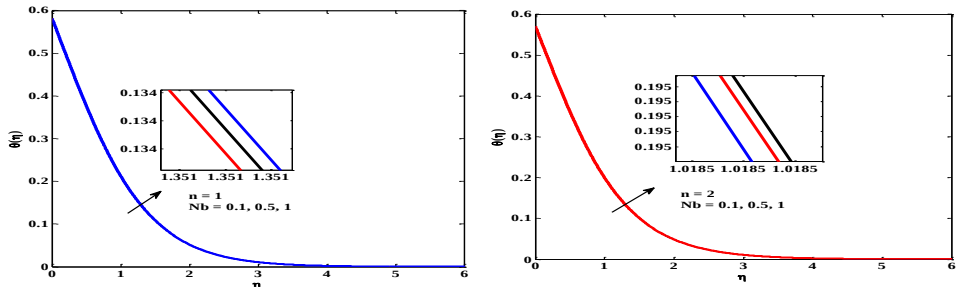

Fig. 16(a), 16(b).Temperature profile for *Nb*.

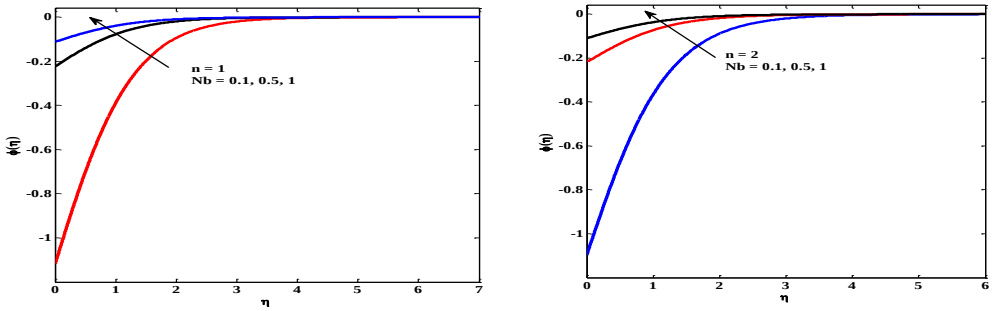

Fig. 17(a), 17(b).Concentration profile for *Nb*.

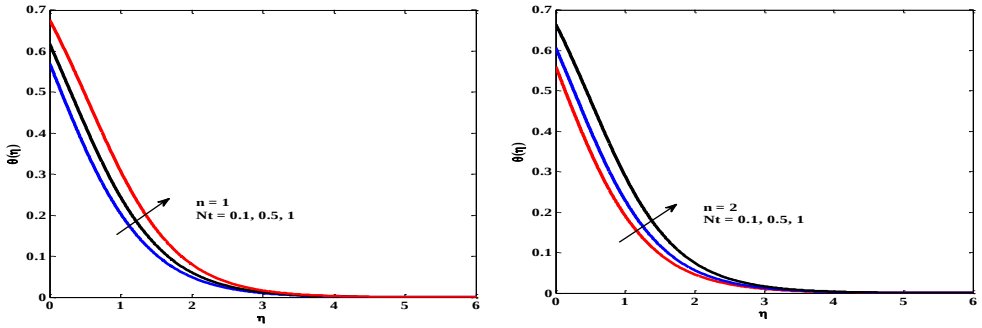

Fig. 18(a), 18(b). Temperature profile for *Nt*.

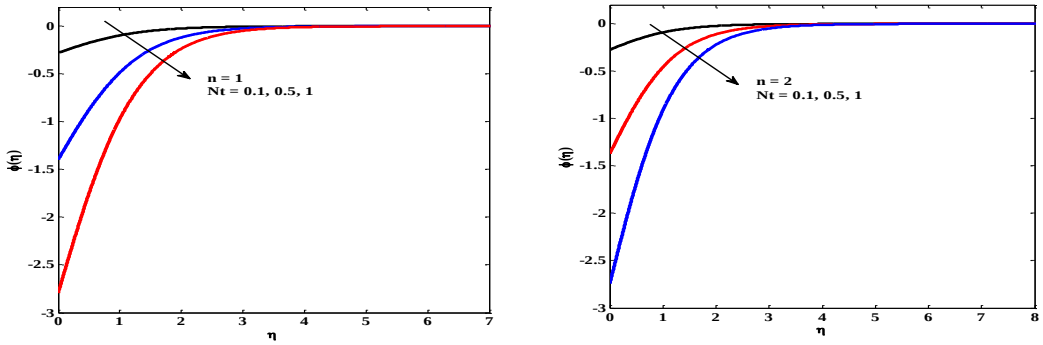

Fig. 19(a), 19(b). Concentration profile for *Nt*.

International Journal of Engineering Research & Technology (IJERT)
ISSN: 2278-0181
Vol. 12 Issue 07, July-2023

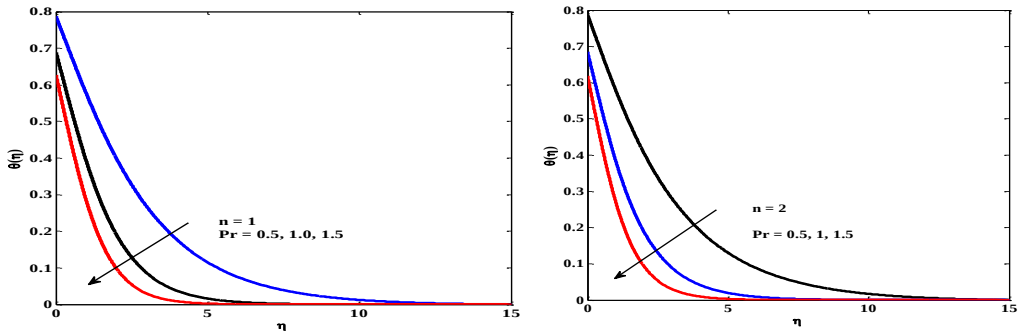

Fig. 20(a), 20(b).Temperature profile for *Pr*.

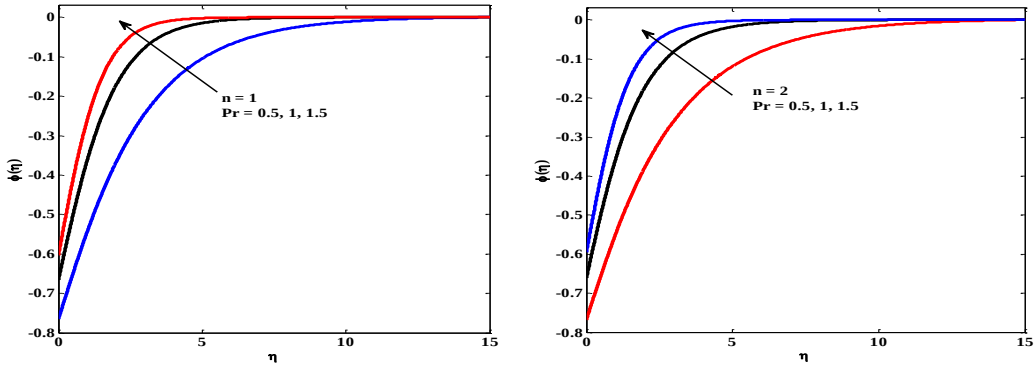

Fig. 21(a), 21(b).Concentration profile for *Pr*.

Table II. Computed values of Skin friction, local Nusselt number and local Sherwood number for various values of *A*, *s*, *M*, *Pr*, *Nb*, *Nt*, *Le*, *γ*.

A	*s*	*M*	*Pr*	*Nb*	*Nt*	*Le*	γ	Skin Friction		Nusselt Number		Sherwood number	
								n = 1	*n* = 2	*n* = 1	*n* = 2	*n* = 1	*n* = 2
0								1.043420	0.524609	0.506808	0.524609	0.655503	0.674587
0.5								0.508063	0.528855	0.508063	0.528855	0.656297	0.677105
1.0								0.508938	0.531149	0.508938	0.531149	0.656816	0.678363
	0.5							0.487823	0.528855	0.487823	0.528855	0.644711	0.677105
	1.0							0.498985	0.578240	0.498985	0.578240	0.651512	0.723403
	2.0							0.508063	0.641128	0.508063	0.641128	0.656297	0.777215
		0.6						0.358977	0.376187	0.358977	0.376187	0.509204	0.529714
		1.2						0.408225	0.427078	0.408225	0.427078	0.560636	0.581874
		1.8						0.445687	0.465489	0.445687	0.465489	0.597788	0.619150
			0.7					0.520274	0.540504	0.520274	0.540504	0.565615	0.585013

International Journal of Engineering Research & Technology (IJERT)
ISSN: 2278-0181
Vol. 12 Issue 07, July-2023

1.0				0.470333	0.492751	0.470333	0.492751	0.588311	0.608107
1.3				0.404991	0.429689	0.404991	0.429689	0.769423	0.791882
	0.1			0.521690	0.541753	0.521690	0.541753	0.720508	0.765513
	0.5			0.461936	0.484820	0.461936	0.484820	0.743419	0.772041
	1.0			0.373833	0.398048	0.373833	0.398048	0.610367	0.629609
		0.1		0.091858	0.092432	0.091858	0.092432	0.656297	0.677105
		0.5		0.341001	0.349793	0.341001	0.349793	0.625834	0.644652
		1.0		0.508063	0.528855	0.508063	0.528855	0.576157	0.594105
			1.2	0.532348	0.552058	0.532348	0.552058	0.111442	0.111704
			1.5	0.518463	0.538964	0.518463	0.538964	0.425294	0.433397
			2.0	0.508063	0.528855	0.508063	0.528855	0.656297	0.677105
				0.1	0.508063	0.528855	0.508063	0.528855	0.623299	0.644680
				0.5	0.507672	0.528432	0.507672	0.528432	0.637221	0.658405
				1.0	0.507494	0.528225	0.507494	0.528225	0.656297	0.677105

4. CONCLUSIONS:

A numerical study was investigated for the mixed convection MHD boundary layer flow of a Sisko nanofluid over a nonlinear permeable stretching sheet with the help of efficient numerical shooting technique with a fourth order Runge-Kutta scheme along with shooting method. Following conclusions give the brief results of the present study.

1) Increase in the values of magnetic parameter decreases the velocity profile for both the power-law index $n = 1$ and $n = 2$.

2) Increase in nonlinear stretching parameter s decreases the velocity and temperature profiles for both the power-law index $n = 1$ and $n = 2$.

3) It is found that larger values of Biot number (γ) lead to increase the velocity and temperature profiles for the power-law index $n = 1$ and $n = 2$.

4) Temperature is enhanced for the higher values of Brownian motion parameter (*Nb)*, Thermophoresis parameter *(Nt)* for the power-law index $n = 1$ and $n = 2$.

5) Concentration profile is decreases by increasing the values of Brownian motion parameter (*Nb)*, Thermophoresis parameter *(Nt)* for the power-law index $n = 1$ and $n = 2$.

5) Increase in the material parameter reduces the temperature for the power-law index $n = 1$ and $n = 2$.

6) Velocity and concentration profiles are increases by the larger values of material parameter for the power-law index $n = 1$ and $n = 2$.

7) Concentration is enhanced for the higher values of Lewis number for the power-law index $n = 1$ and $n = 2$.

International Journal of Engineering Research & Technology (IJERT)
ISSN: 2278-0181
Vol. 12 Issue 07, July-2023

REFERENCES:

[1] Magyari, E. and Keller, B. (2000) Exact Solutions for Self Similar Boundary Layer Flows Induced by Permeable StretchingWalls. European Journal of Mechanics B—Fluids, 19, 109-122.
[2] Gupta, P.S. and Gupta, A.S. (1977) Heat and Mass Transfer on a Stretching Sheet with Suction or Blowing. Canadian Journal of Chemical Engineering, 55, 744-746.

[3] Vajravelu, K. (2001) Viscous Flow over a Nonlinearly Stretching Sheet. Applied Mathematics and Computation, 124, 281-288.
[4] Bhargava, R., Sharma, S., Takhar, H.S., Beg, O.A. and Bhargava, P. (2007) Numerical Solutions for Micropolartransport Phenomena over a Nonlinear Stretching Sheet. Nonlinear Analysis Modeling and Control, 12, 45-63. [Citation Time(s):1]
[5] Prasad, K.V., Vajravelu, K. and Datti, P.S. (2010) Mixed Convection Heat Transfer over a Non-Linear Stretching Surface with Variable Fluid Properties. International Journal of Non-Linear Mechanics, 45, 320-330.
[6] N. Kishan And P. Amrutha , "Effects of viscous dissipation on MHD flow with heat and mass transfer over a stretching surface with heat source, thermal stratification and chemical reaction", Journal of Naval Architecture and Marine Engineering,7(1), 2011, 11–18..
[7]HunegnawDessie , NaikotiKishan, MHD effects on heat transfer over stretching sheet embedded in porous medium with variable viscosity, viscous dissipation and heat source/sink, Ain Shams Engineering Journal (2014) 5, 967–977

[8]SrinivasMaripala, KishanNaikoti, MHD effects on micropolarnanofluid flow over a radiative stretching surface with thermal conductivity, Advances in Applied Science Research, 2016, 7(3):73-82.

[9] Gireesha, B. J.; Mahanthesh, B.; Gorla, Rama Subba Reddy, Suspended Particle Effect on Nanofluid Boundary Layer Flow Past a Stretching Surface, journal of nanofluids, 2014, Vol. 3, pp. 267-277(11)

[10] Sisko AW. The flow of lubricating greases. IndEngChem Res 1958;50(12):1789–92.

[11] Khan M, Shahzad A. On boundary layer flow of Sisko fluid over stretching sheet.QuaestionesMathematicae 2013;3:137–51.
[12] Malik R, Khan M, Munir A, Khan WA. Flow and heat transfer in Sisko fluid with convective boundary condition. PLoS ONE 2014;9(10):e107989.
[13] Khan M, Malik R, Hussain M. Nonlinear radiative heat transfer to stagnation-point flow of Sisko fluid past a stretching cylinder. AIP Advances, 6. 2016. p. 055315.
[14] Malik MY, Hussain A, Salahuddin T, Awais M, Bilal S. Numerical solution of Sisko fluid over a stretching cylinder and heat transfer with variable thermal conductivity. J Mech 2016;32(5).
[15] Choi, S.U.S. (1995). Enhancing thermal conductivity of fluids with nanoparticles. ASME Fluids Eng. Division, 231, 99–105.
[16] Xuan, Y. and Li, Q. (2003). Investigation on convective heat transfer and flow features of nanofluids. J. Heat Transfer, 125, 151-155.
[17] Khan, W.A. and Pop, I. (2010). Boundary-layer flow of a nanofluid past a stretching sheet. Int. J. Heat Mass Transfer, 53, 2477–2483.
[18] Makinde, O.D. and Aziz, A. (2011). Boundary layer flow of a nanofluid past a stretching sheet with convective boundary condition. Int. J. Therm. Sci. , 50, 1326– 1332.
[19] Ishak, A. Nazar, R. and Pop, I. (2009). Boundary layer MHD flow and heat transfer over an unsteady stretching vertical surface. Meccanica, 44, 369 - 375.

International Journal of Engineering Research & Technology (IJERT)
ISSN: 2278-0181
Vol. 12 Issue 07, July-2023

[20] Nadeem, S. Haq, R. Ul and Khan, Z. H. (2014). Heat transfer analysis of water-based nanofluid over an exponentially stretching sheet. Alexandria Eng. J., 53, 219-224.

[21] Nayak M.K. (2016). Thermal radiation effect on MHD 3D flow and heat transfer of nanofluid past a shrinking surface.AMSE J. Modelling B, 85(1), 43-62.

[22] Murthy, P.V.S.N. Reddy, Ch. Ram Chamkha, A. J. and Rashad, A.M. (2013). Magnetic effect on thermally stratified nanofluid saturated non-Darcy porous medium under convective boundary condition. Int. Commn. Heat Mass Transfer, 47, 41–48.

[23] Ibrahim, W., Shankar, B., Nandeppanavar, M.M., 2013. MHD stagnation point flow and heat transfer due to nanofluid towards a stretching sheet. Int. J. Heat Mass Transfer 56, 1–9

[24] Seddeek, M.A., 2003. Effects of radiation and variable viscosity on a MHD free convection flow past a semi-infinite flat plate with an aligned magnetic field in the case of unsteady flow. Int. J. Heat Mass Transfer 45, 931–935

[25] Turkyilmazoglu, M., 2012. Exact analytical solutions for heat and mass transfer of MHD slip flow in nanofluids. Chem. Eng. Sci. 84, 182–187.

[26] Kumaran, V., Banerjee, A.K., Kumar, A.V., Vajravelu, K., 2009. MHD flow past a stretching permeable sheet. Appl. Math. Comput. 210, 26–32.

[27] Raptis, A., Perdikis, C., Takhar, H.S., 2004. Effects of thermal radiation on MHD flow. Appl. Math. Comput. 153, 645–649

[28] Masood Khan, Rabia Malik, AsifMunir, WaqarAzeem Khan, Flow and Heat Transfer to SiskoNanofluid over a Nonlinear Stretching Sheet,

[29] Khan WA, Pop I (2010) Boundary-layer flow of a nanofluid past a stretching sheet. Int J Heat Mass Transf 53 2477–2483.

[30] Wang CY (1989) Free convection on a vertical stretching surface. J Appl Math Mech (ZAMM) 69 418–420.

[31] Gorla RSR, Sidawi I (1994) Free convection on a vertical stretching surface with suction and blowing. ApplSci Res 52 247–257.